ingegneria sismica
International Journal of Earthquake Engineering
Anno XLIII - Num. 2 - 2026

Optimal capacity design and energy efficiency analysis of wind-solar energy storage complementary system based on particle swarm algorithm

Chenguang Zhu[1], *Min Gao*[1,*], *Xiaojun Si*[1], *Qunwei Gao*[1] *and Weizhe Sun*[1]

[1] Pinggao Group Co., LTD., Pingdingshan, Henan, 467000, China

SUMMARY: *In this research work, a two-layer optimization model is established for the energy storage arrangement and the economical operation of the wind-solar combined power generation system. The goal of this model is to describe the mutual connection between the planning and the running of the energy storage system in the process of its capacity configuration optimization. The top layer of the model owns one single optimization goal, which is to cut down the overall whole life-circle cost of the energy storage system.At the same time, the goal of the lower-layer optimization is to cause the overall daily economic income in the process of system operation to reach maximum. For solving the two-layer optimization model, we hence put forward one enhanced self-adaptive forbidden annealing particle swarm algorithm. The viability of this algorithm is through the carrying out of tests on several famous test functions to be assessed.After this, the behavior result of the promoted algorithm is made comparison with that of the Particle Swarm Optimization (PSO) method, therefore, the algorithm's better performance is confirmed. At last, through choosing the X large-scale new-energy base to be the research object, an evaluation is carried out on the optimized operation of the energy-storage battery. This evaluation is conducted in the situation that the configured energy-storage volume is 10 megawatts (MW) and the stored energy is 20 megawatt-hours (MWh).Furthermore, we have carried out an inquiry regarding the connection between the pure incomes obtained from energy-storage investment and the change in the rated capability of the energy storage. After we have completed the evaluation of the results, it is very clear that a bigger energy-storage volume arrangement is not certainly better. When the optimal disposition capacity of the new-energy base is 50 megawatt-hours and the ratio of energy-storage disposition takes up 11.47% of the new-energy installed capacity, hence the benefits reach their maximum.*

KEYWORDS: *wind-solar energy storage complementary system; capacity optimal allocation; IATAPSO algorithm; two-layer optimization model*

1 Introduction

Along with the continuous decrease of fossil fuel storage and the aggravation of global warming, renewable energy has already become a key strategic field that all countries in the whole world are competing to develop [1, 2]. As the comparatively good developed renewable energy choices, wind force and sunlight electric power, have been widely used worldwide [3]. Among them, wind power generation stands out for its safety, non-pollution and energy-abundance characteristics, and its installed capacity is rapidly expanding [4]. Photovoltaic (PV) power

*15155011439@163.com
https://doi.org/10.65102/is2026580
Published: 30 April, 2026

generation, on the other hand, it uses photovoltaic cells for the conversion of light energy into electric power. This thing has obtained much attention because of its good points that it is environment-protective, noiseless, and possesses already fully developed technology [5]. In conclusion, as wind electricity generation technology and solar electricity generation technology continuously make progress and the expense of their use steadily goes down, renewable energy hence will become the core development route for the world's future energy situation.

When making contrast with independent photovoltaic and wind electricity production, the wind-solar mixed system shows better characteristics of mutual compensation [6]. However, because of the circumstance that wind turbine units and photovoltaic electricity production have a restricted rotation inertia support, poor power generation system anti-interference ability, power fluctuation fast, stochastic and other characteristics, beside the problem that the wind-solar complementary system is restricted by natural environment conditions, this brings about the unpredictability and great randomness of electricity production in the wind-solar combined system. Therefore, the grid-connection volume of new energy electricity production is reduced, hence bringing about economic losses on account of wind abandoning and solar abandoning [7-11]. The energy storing device can act as an assisting power source for the wind-solar mixing system. When wind and solar energy have abandonments, it lets electric power be stored by the mode of chemical energy. In the periods of peak load, the energy storage equipment can change the chemical energy back to become electrical energy. This has the function of reducing the speed of load lack and promoting the stable property of the system. [12-14]. The purpose of this multi-energy mutual supplementing is to utilize the largest amount of renewable energy sources at the same time as satisfying energy demands. This paper's goal is to reach high-efficiency energy use and cut down carbon emissions to the smallest degree [15, 16]. This system's internal capacity allocation refinement possesses quite notable research value. Through the carrying out of this method, it can be possible to promote the utilization rate of renewable energy resources and increase the economic benefits of electricity generation factories. At the same time, it makes contribution to the reduction of carbon discharge.

From history beginning until today, very many academic research workers have carried out researches on the capacity distribution problem of energy storage inside the wind-solar complementary system.Zhu et al [17] proposed an optimal configuration one model which is used for grid-connected wind and solar mixed energy storage system is built by us through the utilization of MATLAB/Simulink software. The purpose is to attain the most excellent capacity disposition through simulating a mechanism of optimization. This system is constructed on the basis of a static reactive power compensation device and a conduction-fuzzy dual-mode control approach.But, this simulation-based optimization process has no effect, and therefore it has difficulty satisfying the demands of the fast development of the system. Hou and [18]his work group utilized a cat group optimization algorithm to solve the optimal capability distribution model of a wind-photovoltaic-energy storage system which contains a gravitational energy storage system. They pointed out that this gravity-relied mixed system possesses bigger advantages when it is placed in mountain areas.Ma and [19]his research group used a sparrow searching algorithm to construct a capability distribution optimization model for a mixed wind-solar-energy storage electric power generation system. As the result, it has realized one year cost cut of 91.58 million Chinese Yuan and lowered the abandoning ratio of renewable energy. Liu et al [20] introduced Gray Wolf optimization algorithm is utilized by researchers to achieve the capability distribution optimization of the wind-photovoltaic-storage system inside a park microgrid, the life-cycle carbon emissions have been considered. This algorithm brings about a lowering of the entire yearly cost by 1.2307 billion RMB and a cutting down of carbon emissions by 1,279,979 tons.Zheng and[21] his work group have completed a mixed wind-

solar energy save model. They have utilized the Gray Wolf Pigeon Flock optimized algorithm to carry out optimization on the capacity of mixed wind-solar energy storage systems. This method can play the role of cutting down the expenditures that are connected with the promotion of capacity.Wang et al [22] proposed a capacity optimization strategy for wind-photovoltaic-storage systems with storage battery configurations through an artificial fish swarm algorithm in order to cope with the challenges faced by intermittent renewable energy generation and to optimally reduce the total cost. The above algorithms are difficult to cope with the configuration requirements of wind-optical-storage complementary systems in complex and variable environments, mainly because that they are easy to get local optimal solutions and possess low calculation efficiency.

The Particle Swarm Optimization (PSO) method is one kind of intelligent optimization algorithm which obtains inspiration from the food-seeking behaviors of creatures which live in groups, such as bird kinds and fish. This algorithm has many good points, which include a simple and direct model, convenience for realizing, fast speed of convergence, high accuracy, and very good parallel handling abilities.Wu and [23]his research colleagues put forward an enhanced particle swarm optimization (PSO) method for solving the capacity allocation problem of a wind-photovoltaic-storage integrated power system. They used the technical features of the storage part and the probability of supply break as restriction conditions, and they set the initial capital expenditure as the objective function. Qian and [24] his work group have combined the Genetic Algorithm with the PSO algorithm for carrying out the work of carrying out optimized distribution of the capability of an off-grid wind-solar-storage combined power generation system. They have completed this work through the inspection of data which have relation to investment, maintenance expenditure, and many kinds of reliability restriction conditions. The aim of this conduct was to guarantee the system's stable condition and cut down the expenses of investment and maintenance. Lv et al [25] used PSO to design an optimization method for wind and solar complementary power generation system considering the maximum capacity of renewable energy sources, stating that the maximum capacity of the complementary system is achieved when the installation volume of wind energy and photovoltaic power is respectively 2350 megawatts and 1898 megawatts, correspondingly. Wang et al [26] dynamically adjusted the inertia weight factor of the PSO algorithm to solve the problem of local optimal solution, through the adoption of this method, an optimization model for the capacity distribution of the wind-solar-load energy storage system has been constructed. Therefore, the proportion of wasted wind and solar energy has a decrease of 17.5 percentage points.Jiang et al [27] integrated k-mean algorithm pairs, empirical modal decomposition and dynamically adjusted PSO algorithm to minimize the overall economic cost as the goal, furthermore, an optimization method was brought forward for the capability distribution of the wind-solar-energy-storage system., which reduces the cost and maintains the system stability at the same time. The great part of the documents spoken above puts emphasis on using either one single technical index or one single economic index for the planning of wind energy storage complementary systems. It also carries out analyses upon economic efficiency and stability among different methods. Nevertheless, a not large number of research works have succeeded in realizing the combination of these two aspects. In the actual engineering construction work of storage systems, two kinds of factors all need to be considered by us. Furthermore, the calculation efficiency of the optimized arithmetic methods which are used for the optimization of wind-solar-storage complementary systems needs further promotion. In addition, it is the fact that there exists a very notable lack of research which carries out assessment on the energy efficiency of this system.

This research deals with the problem of carrying out optimal allocation of energy storage volume inside a mixed system which combines wind energy and solar energy storage. Through

the introducing of the concept of life-cycle cost (LCC), a two-tier optimization model has been developed by us. This model includes both the energy storage distribution and the system economic operation. The objective that the upper-level problem has is to make the LCC of the energy storage system become smaller. From another perspective, the lower-level problem takes as its optimization objective the maximization of the daily operation economic benefits of the whole system. For the purpose of strengthening the global searching ability of the particle swarm algorithm, and for avoiding that it falls into the trap of locally optimal solutions, an annealing selecting mechanism that possesses forbidden stimulation functions is put forward. After that, an ameliorated self-adaptive prohibited annealing particle swarm arithmetic is put forward to resolve the two-layer optimization model. For the purpose of carrying out validation on the improved particle swarm algorithm, one test function has been selected. This function is utilized for evaluating the algorithm's possibility of realization and for ascertaining its optimal parameters. Following this step, a comparison which is relevant is conducted between the algorithm that has been improved and the Particle Swarm Optimization (PSO). At the same time, through utilizing the basic datum from a large-scale new energy base (X), the effect of the capacity optimization and distribution method which we put forward for the complementary system that is formed by wind, solar, and energy storage has gotten verification.

2 Capacity optimization allocation method of wind energy storage complementary system

2.1 Basic modeling of wind energy storage complementary system

2.1.1 Wind turbine power generation model

Simplified models of the output power P_m and output mechanical torque T_m of a commonly used wind turbine are, respectively:

$$P_m C_p \rho \pi R^2 v^3 \eta_t \eta_g / 2 \tag{1}$$

$$T_m = P_m / w = 0.5 C_p \rho \pi R^2 v^3 \eta_t \eta_g / w \tag{2}$$

where C_p is the wind energy utilization factor. ρ is the air density. R is the radius of wind wheel. v is the wind speed. η_t is the mechanical efficiency of the transmission. η_g is the mechanical efficiency of the generator. w is the rotational angular velocity.

C_p can be approximated as:

$$C_p = 0.22(116/A - 0.4\beta - 5)e^{-12.5/A} \tag{3}$$

where A is a function of the fan tip speed ratio λ and the pitch angle of the paddle β.

A can be expressed as:

$$A = 1/\left[1/(\lambda + 0.08\beta) - 0.035/\left(\beta^3 + 1\right)\right] \tag{4}$$

In practical engineering, the fan output power (Eq. (1)) can be simplified to Eq. (5):

$$P_{WG}=\begin{cases} C_p\rho\pi R^2 v^3\eta_t\eta_g/2 & v_c\leqslant v\leqslant v_r \\ P_R & v_r\leqslant v\leqslant v_F \\ 0 & v<v_c \text{ or } v>v_F \end{cases} \tag{5}$$

where P_{WG} is the actual output power of the fan. v_c is the fan cut-in speed. v_r is the rated speed of the fan. v_F is the fan cut-out speed. P_R is the rated power output of the fan.

2.1.2 Modeling of photovoltaic cell power generation

Figure 1 gives depiction of the equal electricity circuit that the solar cell uses. I_{PV}, V_{PV} are the output electric current and voltage of the solar cell, respectively. I_{L} is the photogenerated current. I_{D} is the electric current which goes through the diode. I_{sh} is the current flowing across the equivalent shunt resistor. R_{s} is the equivalent series resistance. R_{sh} is the corresponding electric resistance that is parallel.

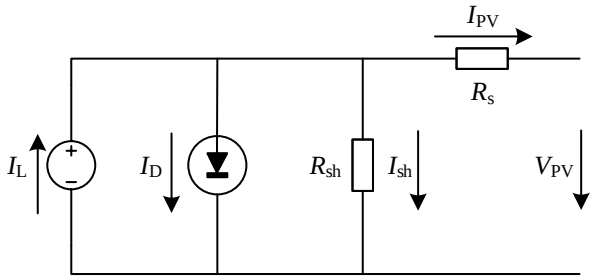

Figure 1: Solar cell equivalent circuit

The current I_{L} is calculated as:

$$I_{\mathrm{L}}=\left[I_{\mathrm{sc}}+k_1\left(T-T_{\mathrm{r}}\right)\right]S/1000 \tag{6}$$

where I_{sc} is the short-circuit electric current of the photovoltaic battery which is under the reference temperature condition. k_1 is the temperature coefficient of short-circuit current. T is the current absolute temperature. T_{r} is the reference temperature. S is the current light intensity.

The expression for the output current I_{PV} is:

$$I_{\mathrm{PV}}=I_{\mathrm{L}}-I_{\mathrm{D}}-I_{\mathrm{sh}} \tag{7}$$

Since I_{sh} is much smaller than I_{PV}, the simplified model is:

$$I_{\mathrm{PV}}=I_{\mathrm{L}}-I_{\mathrm{D}}=I_L-I_0\mathrm{e}^{\left[q(V_{\mathrm{PV}}+I_{\mathrm{PV}}R_{\mathrm{S}})/(AKT)-1\right]} \tag{8}$$

Among them:

$$I_0=I_{\mathrm{s}}\left(t_0\right)2^{\left[(T-T_{\mathrm{r}})/10\right]} \tag{9}$$

where I_0 is the diode reverse saturation current. $q = 1.6 \times 10^{-19}$ C is the electron charge. A is the diode curve factor, $A = 1 \sim 2$. K is the Boltzmann constant, $K = 1.38 \times 10^{-23}$ J / K. $I_s(t_0)$ is the diode reverse saturation current at reference temperature.

Then the PV cell output power P_{PV} is:

$$\begin{aligned} P_{PV} &= I_{PV} V_{PV} \\ &= I_L V_{PV} - I_0 V_{PV} e^{\left[q(V_{PV} + I_{PV} R_S)/(AKT) - 1\right]} \end{aligned} \tag{10}$$

For the promotion of the effect degree of photovoltaic electricity production, the end voltage is carried out regulation to make that the output electricity of photovoltaic cell keeps at its maximum value in every moment V_{PV}, i.e., the maximum power point tracking.

2.1.3 Combined wind power system power generation model

The whole output capability of the wind-solar combined electricity producing system is equal to the sum of the electricity produced by the wind machine and the electricity produced by the solar photovoltaic battery array. The concrete calculation formula is shown below:

$$P(t) = P_{WG}(t) + P_{PV}(t) \tag{11}$$

where $P(t)$ is the output power of the wind-solar co-generation system.

2.2 Description of the problem

A mutually supplementing system of wind and solar energy preservation, which is installed with energy preservation units of a certain capacity, can effectively promote the stability of this system. Therefore, it also helps the local use of renewable energy sources. Even so, the main factor that blocks the progress of the "new energy combine with energy storage" mode is the expense of energy storage. For the reduction of expenditures, from one aspect, the ceaseless perfection and promotion of energy storage technology are needed; On the other hand, the deep-going research regarding optimization of energy storage capability arrangement can be conducted. Although the technology of energy storage has obtained fast development at the present stage, its costs of construction and investment still stay comparatively high, therefore it becomes a difficult thing to get positive profits in the short time. If the short-term return on investment to measure the economy of the system construction will inevitably lack of reasonableness, on the contrary, when one carries out the evaluation of the capital expenditure and profit of an energy storage system, adopting the long-term perspective possesses higher actual significance. Therefore, the carrying out of research on the best distribution of energy storage capacity through bringing into consideration the full-life-cycle cost of energy storage is more scientific in nature and has complete logic.

The whole cost in the whole life cycle of an energy storage system includes the one-time upfront capital spending that is needed for purchasing the main equipment when the system is in its first construction stage. In addition, this includes the operation and maintenance expenditures that are produced after the system is put into operation, together with the expense of equipment renewal and the recovery cost at the conclusion of the project life period. To conduct scientific calculations on the operation and maintenance costs of an energy storage system, one must perform an overall analysis of the system's operation scheme. This analysis aids in determining the energy storage output. Once the output is confirmed, the total life - cycle

cost of the energy storage system can be calculated. Subsequently, based on this calculated cost, the energy storage capacity can be planned.

Considering the mutual interaction between the long - term strategic plan and short - term operation situations of the energy storage system, a two - layer optimization method is highly suitable for solving the energy storage planning problem. In this research paper, a two - layer optimization model for the deployment and operation of the energy storage system is established, and the transfer relationship between the upper and lower optimization decision variables is shown in Fig. 2. The decision variables in the upper - layer planning model are the power and capacity configuration of the energy storage system, with the objective of minimizing the entire life - cycle cost of the energy storage. The decision variables of the lower - layer operation model are the real - time output power of each controllable unit in the wind - storage multi - energy complementary system during daily operation. Specifically, the charge - discharge power of the energy storage system and the amount of purchased electricity are considered to maximize the daily economic benefits of the system. In the two - layer optimization process, the upper - layer planning model transfers the optimal energy storage configuration scheme to the lower - layer operation model. In turn, the lower - layer operation model sends the optimal system operation plan to the upper - layer planning model.

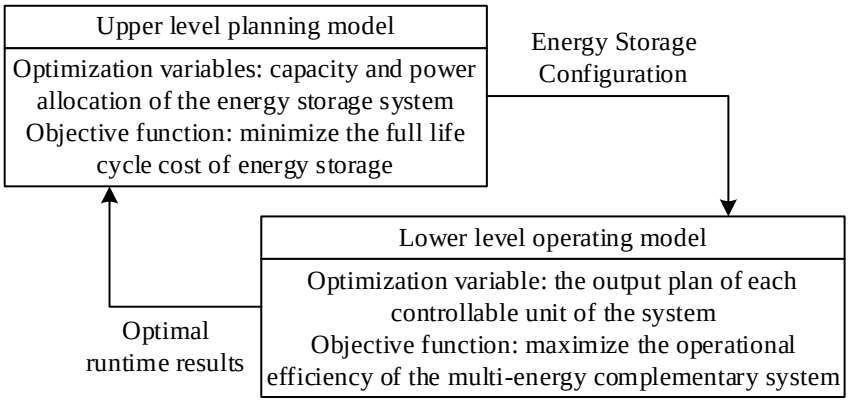

Figure 2: Model framework for double layer optimization

2.3 Modeling

2.3.1 Upper layer model

In the two-level optimization model of energy storage configuration and system economic operation developed in this chapter, the decision variables of the high-level optimization planning model are the capacity and power settings of the energy storage system. The optimization objective is to minimize the equivalent annual cost of the energy storage system over its entire life cycle. The life-cycle expense (LCE) of the energy storage system represents the total sum of all relevant costs and expenditures that occur during the system's entire life cycle, from its design and commissioning to its end-of-life reuse. It mainly consists of four types of costs: the initial investment cost (IC), the operation and maintenance cost (OC), the equipment replacement cost (RC), and the end-of-life recovery cost (DC). Therefore, the objective function of the high-level optimization can be formulated as follows:

$$\min LCC = IC + OC + RC + DC \tag{12}$$

(1) Initial investment cost

The upfront input cost of the energy storage system refers to the fixed capital invested during the early stage of system construction for the purchase of major equipment.The expense that we put into investment is:

$$IC_1 = c_1 E_{rate} + c_2 P_{rate} + c_3 E_{rate} \tag{13}$$

c_1 - Unit capacity cost of the system.

c_2 - Cost per unit of power of the system.

c_3 - the expenditure for each unit of capability of the additional establishments.

E_{rate} - the configured capacity of the system.

P_{rate} - the configured power of the system.

The cost of the annual value of the initial investment, etc. is:

$$IC = C(r,n)\left(c_1 E_{rate} + c_2 P_{rate} + c_3 E_{rate}\right) \tag{14}$$

where $C(r,n)$ is the coefficient of equal annual values:

$$C(r,n) = \frac{r(1+r)^n}{(1+r)^n - 1} \tag{15}$$

r - baseline discount rate.

n - project period.

(2) Operation and maintenance cost

The expense relevant to the running and maintenance of the energy storage system belongs to the dynamic costs that it produces in the whole operation period to ensure its normal work. According to if the cost is produced in relation to the particular working procedure,the operation and maintenance costs can be divided into two types: fixed and variable. The operation and maintenance expenses of the energy storage system are presented on an annual basis.

$$OC = c_4 P_{rate} + \beta Q \tag{16}$$

$$Q = D\sum_{t=1}^{24} \left| P_{ES}(t) \right| \tag{17}$$

c_4 - annual fixed expenditure on the system's operation and maintenance for every unit of power. β - coefficient of variable charging and discharging cost per unit of the system.

D -the sum total of days inside one whole year on which the energy storage system is carrying out operation.

Q - the total annual charge/discharge amount of the energy storage.

$P_{ES}(t)$ - the charging and discharging power of the energy storage at time t in the daily optimized operation strategy of the multi - energy complementary system.

(3) Equipment replacement cost

The cost of each replacement of battery energy storage during the project cycle is:

$$RC_1 = \left(1-\alpha\right)^{km} c_1 E_{rate} \tag{18}$$

α - average yearly speed at which the capital input of the energy storage system goes down.

m - battery energy storage life cycle.

k - the number of battery body replacements, $k = n/m - 1$, when k is a non-integer, k is rounded up by 1.

Therefore, he annual equal value of the substitute expense for the energy storage system is just as below:

$$RC = c_1 E_{rate} \sum_{L=1}^{k} \frac{(1-\alpha)^{Lm}}{(1+r)^{Lm}} C(r,n) \tag{19}$$

L - Lth replacement of the battery body.

(4) End-of-life recovery cost

In the whole process of the project, the cost for taking back the energy storage system when its life comes to the end includes two parts: the cost of end-of-life disposal and the leftover value obtained from recycling. Therefore, the end-of-life recovery expense of the energy storage, which is expressed as an equivalent annual numerical value, hence is just as follows:

$$DC = \left(c_p P_{rate} + c_c E_{rate}\right) C\left(r,n\right)\left(1+r\right)^n - c_{res}\left(IC + RC\right) \tag{20}$$

c_p - system unit power end-of-life treatment cost.

c_c - system end-of-life treatment cost per unit of capacity.

c_{res} - system recovery salvage rate.

Upper level constraints:

(1) Restrictions on nominal power and volume for the collocation of energy storage systems:

$$P_{rate} \le P_M \tag{21}$$

$$E_{rate} \le E_M \tag{22}$$

P_M - Energy storage maximum power.

E_M - maximum capacity of energy storage.

(2) Energy storage system charging and discharging power limits:

$$P_{rate} \ge \left|P_{ES}(t)\right| \tag{23}$$

$P_{ES}(t)$ - the charging and discharging power of the energy storage in the 24-hour t time period.

(3) Energy storage system charge state constraints

By restricting the charge-discharge depth of the energy storage system, the service life of energy storage devices can be effectively prolonged. The charge and discharge degree of the energy storage system can be represented by the state of charge (SOC), and the specific restrictions are as follows:

$$E_{rate} \ge \frac{1}{SOC_{\max} - SOC_{\min}} \sum_{t=1}^{j} \delta(t) P_{ES}(t) \Delta t \tag{24}$$

$$\delta(t)=\begin{cases}\eta_c & P_{ES}(t)\le 0\\ \dfrac{1}{\eta_d} & P_{ES}(t)>0\end{cases} \tag{25}$$

j - calculate the time period $j=1,2,...,24$.

$SOC_{\max}$ - the highest charge state permitted for the system.

$SOC_{\min}$ - the lowest charge state allowed by the system.

Δt - the time interval between the t time period and the $t+1$ time period.

η_c - Charging efficiency of the system.

η_d - Discharge efficiency of the system.

2.3.2 Lower level model

The lower-level optimization problem aims to optimize the daily output strategy for the economic operation of the wind energy storage and complementary system. The optimization objective is to maximize the daily operational economic benefit of the system by optimizing the real-time output plan of each controllable unit in the multi-energy system (MES), specifically the charging and discharging power of the storage system and the amount of purchased power. Based on the predicted data of wind and solar power generation for the next day, along with the electricity load demand, the entire system is ensured to operate safely and stably. Here, the revenue consists of the earnings from selling power from the system to the load side and the income from government subsidies. Meanwhile, the expenditures include the system's operation and maintenance costs, power generation costs, and electricity purchase costs.

In summary, the economic benefit F of one day of system operation is as follows:

$$\max F=\sum_{t=1}^{23}\left(\gamma_t P_{load}(t)+\sum_{i=1}^{1}k_i P_i(t)-\beta\left|P_{ES}(t)\right|-\alpha_t P_G(t)\right)-\sum_{i=1}^{3}C_i \tag{26}$$

γ_t --The price of electricity sold by the system to the load terminals during this t time period.

i - $i=1,2,3$ represents wind power, solar-electric electricity and energy storage devices, respectively.

k_i - government-subsidized price standards for the production of wind and solar energy electricity.

β - the cost coefficient that belongs to the system's charge and discharge on each unit basis.

α_t - the tariff of power purchased from the grid by the system in t time period.

$P_{load}(t)$ - the electricity load of the system in t time period.

$P_i(t)$ - the power generated by the generation system i in time period t.

$P_{ES}(t)$ -the strength that energy storage device carries out charging and discharging at a concrete time t.

$P_G(t)$ - the electric energy that the system obtains from the power network on a concrete time point t.

C_i - the daily operation and maintenance cost of i the generation system.

Lower level constraints:

(1) System power balance constraints

To ensure system safety and equipment service life, we regard the balance between supply and demand as a strict constraint. Based on the power balance constraints, the following equation can be derived:

$$P_{PV}(t)+P_{wind}(t)+P_G(t)+P_{ES}(t)=P_{load}(t) \tag{27}$$

$P_{PV}(t)$ --Photovoltaic power at time t.

$P_{wind}(t)$ - wind generation power in t time period.

(2) Output constraints for each unit

For the guarantee of the security and the stability of the system's operation work, every power generation system is subjected to strict upper limit and lower limit restrictions. We do not obtain and bring into consideration the maximal and minimal digital values of the electric power that passes through the contact wire.

$$P_i^{\min} \le P_i(t) \le P_i^{\max} \tag{28}$$

The superscripts $\max$ and $\min$ represent the maximum and minimum output power of each generation system, respectively.

(3) Limitations upon the charging condition of the energy storage system

In the upper - layer optimization model, there are restrictions on the operating conditions of the energy storage system's load. Similarly, in the lower - level model, it is essential to impose constraints on the operating state of the energy storage system's load.

$$SOC(t)=\begin{cases}(1-\omega)SOC(t-1)-\dfrac{\eta_c P_{ES}(t)\Delta(t)}{E_{rate}} & P_{ES}(t)\le 0\\ (1-\omega)SOC(t-1)-\dfrac{P_{ES}(t)\Delta(t)}{\eta_d E_{rate}} & P_{ES}(t)>0\end{cases} \tag{29}$$

$$SOC_{\min} \le SOC(t) \le SOC_{\max} \tag{30}$$

$SOC(t)$ - the electricity bearing situation of the battery in one established time point t.

$SOC(t-1)$ -the electricity quantity that is inside the battery at one definite time point. $t-1$.

ω - self-discharge coefficient of the battery.

E_{rate} - rated capacity of the battery.

η_c - the efficiency degree of the energy storage system in the proceeding of charging.

η_d -the efficiency of energy release from the energy storage system.

2.4 Model solving for improved adaptive forbidden annealing particle swarm algorithm

Due to the significant differences in the output characteristics of each power generation system, the problem of energy storage capacity distribution exhibits multiple variables, numerous constraints, high nonlinearity, complexity, and uncertainty. Therefore, a smart optimization method is required to address this issue. An enhanced particle swarm algorithm is employed to

solve the two - layer optimization model of energy storage allocation and the system's economic operation.

Obtaining inspiration from the collective motion rules of bird kinds, the Particle Swarm Algorithm (PSO) has been proposed by researchers. PSO is one probability type search algorithm, which has characteristics of fast convergence speed and the ability that it can carry out overall search in whole solution space.Assume that N particles form a population in a D-dimensional search space, and each particle is a D -dimensional vector $x_i = \left[x_{i1}, x_{i2}, \cdots, x_{iD}\right], i = 1, 2, \cdots, N$. Its velocity vector is: $v_i = \left[v_{i1}, v_{i2}, \cdots, v_{iD}\right]$. The i th particle individual optimal position $pb_i = \left[p_{i1}, p_{i2}, \cdots, p_{iD}\right]$. The particle swarm optimal position $gb = \left[g_1, g_2, \cdots, g_D\right]$. Each particle vector can serve as a potential solution to the optimization problem. In the Particle Swarm Optimization (PSO) algorithm, particles undergo an update process.

$$\begin{aligned} v_i^{t+1} &= \omega v_i^t + c_1 r_1 \left(pb_i^t - x_i^t \right) + c_2 r_2 \left(gb^t - x_i^t \right) \\ x_i^{t+1} &= x_i^t + v_i^{t+1} \end{aligned} \tag{31}$$

where: v_i^t, x_i^t are the velocity vector and position vector of the i th particle iteration t , respectively, and so on. pb_i^t, gb^t are the individual optimal position of the i th particle for the t th iteration, and the global optimal position of the t th iteration, respectively. ω is the inertia weight coefficient. c_1, c_2 are the individual and population learning factors, respectively, which are important parameters to control the iteration. r_1, r_2 are random numbers between $[0,1]$.

2.4.1 Improving the parameter adaptive strategy

In the conventional particle swarm optimization algorithm, the parameters ω, c_1 and c_2 play a core role in the control of the direction of particle movement. In the most part of these algorithms, these parameter numerical values are generally decided according to experience knowledge. But, these pre-fixed numerical values have difficulty in satisfying the requirements of each different iteration stage.

(1) Inertia coefficient tangent function control strategy

The inertia coefficient ω is used for quantifying the degree to which the speed of last generation is inherited, hence it has a direct influence upon the searching ability of the algorithm. When the coefficient ω is comparatively big, the present condition is remarkably affected by the moving speeds of the last-generation particles. Therefore, the particles carry out movement with high velocity and have a strong whole-range search ability. But, the obtaining of local convergence has become one difficult problem under this circumstance. On the opposite side, when the coefficient ω has a small value, the effect coming from particles of the previous generation is of the smallest degree. Under this kind of circumstance, the algorithm therefore has a tendency to carry out the concentration on the detailed local search works. It is a pity that this situation frequently causes the algorithm to be stuck in partial extreme values, hence bringing about outcomes that are not the best solutions. According to these characteristics, a control method for the coefficients, which is based on the inverse tangent function, is proposed.

$$\omega = -\frac{\left(\omega_{\max} - \omega_{\min}\right)}{2} \times \frac{\arctan[t/n - M/(2n)]}{\arctan[M/(2n)]} + \frac{\left(\omega_{\max} + \omega_{\min}\right)}{2} \tag{32}$$

where: $\omega_{\min}, \omega_{\max}$ are the lowest and highest numerical values of the designated inertia coefficient, respectively. t, M are the current and the given maximum number of generations, respectively. n is the attenuation coefficient. The larger n is, the faster its medium-term decay rate is, and vice versa.

In the beginning stage of the algorithm, ω is held at a big scope to enhance the global searching ability and stop being caught in local minimum points.In the middle stage, you must keep a fixed speed to continuously reduce the size of ω for incrementally promoting its ability on local searching.In the later stage, the value of ω is smaller. A lower numerical value allows for a thorough and detailed investigation of the region surrounding the extreme value.Therefore, the particles have gradual movement toward the global optimal position. An adaptive strategy can be employed to balance the global and local searching abilities. (2) Cosine function control strategy for the learning factor.

For the learning factor c_1, c_2, if c_1 is larger,the particle individuals move toward their respective optimal positions, thus the whole collective's global searching ability is strengthened. However, therefore, it still has difficulty to find the best value and make convergence get realized. If c_2 is larger, it displays a fast convergence speed, nevertheless, it possesses the tendency to be caught in local maximum values. Therefore, a method for the nonlinear research factor which is established on the cosine function is now being used:

$$c_1 = 1.3 + 1.2\cos(\pi \times t / M) \tag{33}$$

$$c_2 = 2.0 - 1.2\cos(\pi \times t / M) \tag{34}$$

In the starting stage of this algorithm, $c_1 = 2.6, c_2 = 0.9$, and as the number of iterations t increases, c_1 gradually decreases to 0.1, and on the contrary, c_2 it continuously ascends to a level which is 3.5.This kind of disposition can guarantee that the ability of global search work in the first stage. In addition, the speed of change is comparatively slow, therefore it allows the carrying out of a more comprehensive investigation of the whole world. In the middle and late stages c_1 decreases rapidly and c_2 rises rapidly, resulting in a rapid increase in the local search capability and accelerated convergence.

2.4.2 Improving the forbidden annealing perturbation strategy

In the evolution course of particle swarms, the algorithm obtains a certain degree of overall searching ability through the parameters that can adapt themselves.Even so, its ability of global search has limitation. When particles are processed by repeated computations, it is an extremely great difficulty to stop very many particles from gathering together. This therefore leads to a shortage of particle variety. Furthermore, the phenomenon of "pre-mature gathering convergence" which is caused by the gathering of many particles appears in the early and middle periods of iteration. Because of this, the algorithm has the tendency of being caught in partial optimal solutions. To get rid of the local extreme value only through renewing the positions of particles in accordance with equation (31) is a thing of great difficulty.It is not difficult at all for people to get caught into the condition of localization. Furthermore, hence only depending on carrying out position renewal through Equation (31), this makes the getting rid of local extreme value become very difficult. The selection mechanism of forbidden excitation annealing is given, Furthermore, one ameliorated self-regulating tabu simulated annealing particle swarm optimization algorithm (IATAPSO) is proposed by us for the selection

of the candidate solution of the globally optimal position x_{br} instead of the solution of the global optimal position gb, utilize the probability of its unexpected jump to, to a certain extent, hinder the appearance of a "premature" situation.

(1) Annealing temperature adaptation value

The simulated annealing algorithm, which is a method of overall optimization, obtains its inspiration from the physical annealing phenomenon. This technique makes use of the Metropolis principle, and it carries out strict management on the reduction of temperature, therefore it solves the problem of global optimization. This result is obtained through the integration of the Metropolis rule, its i th particle temperature adaptation value is defined as $T_{fit}(i)$, Furthermore, the method for finding its position is that which follows:

$$T(i)=\begin{cases} e^{-\frac{(pbest(i)-gbest)}{T_e}} & pbest(i)\neq gbest \\ t & pbest(i)=gbest \end{cases} \tag{35}$$

$$T_{fit}(i)=\frac{T(i)}{\sum_{i=1}^{N}T(i)} \tag{36}$$

where $T(i)$ is the worth of the accommodation toward temperature that corresponds to the i particle. $pbest(i)$ is the individual optimal value of the i particle, and the respective optimal position of its corresponding individual particle is pb_i. $gbest$ is the global optimal value, and its corresponding particle global optimal position is gb. T_e is the currently existing algebra which is connected to the annealing temperature, that is firstly chosen and is renewed in the following way:

$$T_c(t)=\begin{cases} gbest/\ln 5, & t=1 \\ K\times T_c(t-1), & t\neq 1 \end{cases} \tag{37}$$

where K is the coefficient of cooling for annealing, which is generally taken to be a value close to 1 between $[0,1]$ and takes the value of 0.9.

(2) Taboo excitation degree

Combined with the idea of forbidden search, the algorithm should avoid too much repetition in the local search at the early and middle stages of the iteration, hence this situation can cause the waste of particles. It ought to record the best global position that the former generation has found out and reduce the work to look for this position in the searching procedure of the later generation. Therefore, the pre-particle renewal undertakes more functions in the whole search process, hence it promotes the integral search capability.

According to the Euclidean distance which lies between each particle, we give "rewards" to those particles which are far away from the global optimum position. $\left(M_{fit}\right)$:

$$D(i)=\sqrt{\sum_{k=1}^{D}\left(x_{i,k}^{t}-gb_k^t\right)^2} \tag{38}$$

$$M_{fit}(i)=\frac{D(i)}{\sum_{i=1}^{N}D(i)} \tag{39}$$

where: $x_{i,k}^{t}$ is the t th iteration of the i th particle in the k th dimension. gb_{k}^{t} is the k th dimension of the t th iteration of the global optimal position. $D(i)$ is the Euclidean distance between the i particle and the global optimal position, and $D(i)$ is normalized to obtain $M_{fi}(i)$.

Furthermore, for the prevention of overmuch harm in the following steps of the repeated process and for the guarantee of the convergence ability of this algorithm, merely the first three particles, which are arranged in order from high to low according to the value of $D(i)$ are considered here for the degree of incentive, while the other particles are not considered and are regarded as having no incentive.

(3) Roulette algorithm to select the perturbation particles

The T_{fti}, M_{fit} are linearly combined and normalized to obtain the overall fitness value:

$$Fit(i)=\frac{T_{fit}(i)+\frac{M-t}{M}\times M_{fit}(i)}{\sum_{i=1}^{N}\left[T_{fit}(i)+\frac{M-t}{M}\times M_{fit}(i)\right]} \tag{40}$$

The particles obtained are the perturbation particles x_{br} by the roulette wheel selection method, which selects among the set of particles pb^{t} according to their overall particle adaptation values. The x_{br} is utilized instead of the gb^{t} particle in Eq. (31) to participate in the particle update:

$$v_{i}^{t+1}=\omega v_{i}^{t}+c_{1}r_{1}\left(pb_{i}^{t}-x_{i}^{t}\right)+c_{2}r_{2}\left(x_{br}-x_{i}^{t}\right) \tag{41}$$

3 Analysis of examples

3.1 Test Functions

In the passed several years, along with computer technology has had steady advancement, modern production ways have more and more had the tendency to rely on computers to replace the traditional handwork production ways. Intelligent algorithms are widely used in production practice because of their autonomous optimization ability and advantages such as high efficiency and high precision, etc. While people continue to develop the application of intelligent algorithms, many new algorithms are also proposed. In this process, for verifying the function of the proposed algorithms and the calculation result of the application, it is necessary that certain standard testing methods are utilized to evaluate these objects.

In the domain of intelligent optimization algorithms, the total goal of an algorithm is to find the extreme value of the objective function that is being optimized.The inside property and degree of complication of this objective function can greatly affect both the optimization procedure and its results. According to the traits and mathematical natures of different optimized functions, many test functions have been proposed. In these, the widely known Benchmark function may be divided into the below classifications:

(1) the test function of the weak correlation between variables, the existence of a small number of local extreme points, with a unique extreme point of this type of test function is a more basic optimization test function, the search difficulty is not high, the more commonly used Sphere function, the expression is:

$$f(x)=\sum_{i=1}^{d}x_i^2 \tag{42}$$

The Sphere function is a standard single-peaked function with no interactions between the variables, and its search space is $-80\le x_i\le 80$, and the optimal solution of the function is: $\min\left(f\left(x_i\right)\right)=f(0)=0$. Figure 3 give display the MATLAB simulation pictorial of this function.

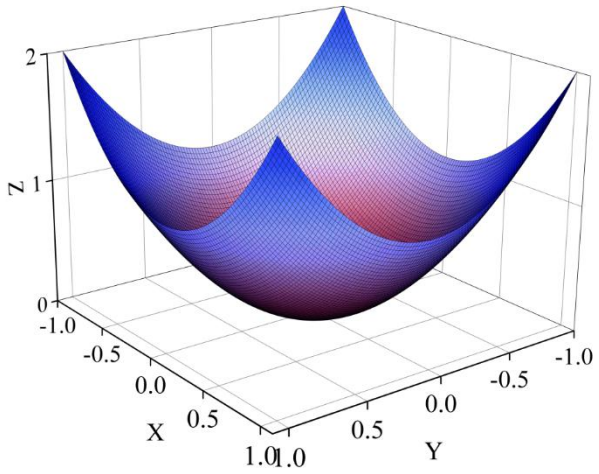

Figure 3: Sphere function

(2) The test function has a strong correlation between the variables, and the distribution of the extreme value is narrow, with a unique extreme value point.

This special type of test function is the single-valley or the multi-valley function. That extreme value is located inside the valley of a limited space. In the algorithm's optimization process, although it is comparatively not difficult to find this region of the space, it is much more difficult to achieve convergence at the unique extreme value point. More commonly used are the Rosenbrock function, whose expression is:

$$f(x)=\sum_{i=1}^{d}\left[100\left(x_i+1-x_i^2\right)^2+\left(x_i-1\right)^2\right] \tag{43}$$

Rosenbrock is a single-peaked pathological function with a search space of $-30\le x_i\le 30$ and the optimal solution of the function is $\min\left(f\left(x_i\right)\right)=f(1)=0$. Its MATLAB simulation image is shown in Fig. 4.

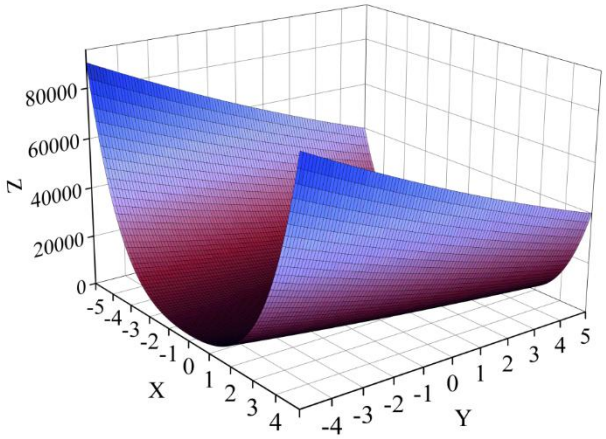

Figure 4: Rosenbrock function

(3) The variable correlation of the test function is weak, there are more local extremes, with a unique extreme point of this type of test function has more local extreme points, therefore, in the process of optimization, the algorithm has the difficulty to converge to the overall maximum value or minimum value.More commonly used are Rastrigin function and Ackley function, etc., of which the expression of Rastrigin function is:

$$f(x)=10d+\sum_{i=1}^{d}\left[x_i^2-10\cos\left(2\pi x_i\right)\right] \tag{44}$$

The Rastrigin function is a multi-peak function which possesses a search space of $-5\le x_i\le 5$, and the optimal solution of the function is: $\min\left(f\left(x_i\right)\right)=f(0)=0$. Its MATLAB simulation image is shown in Fig. 5.

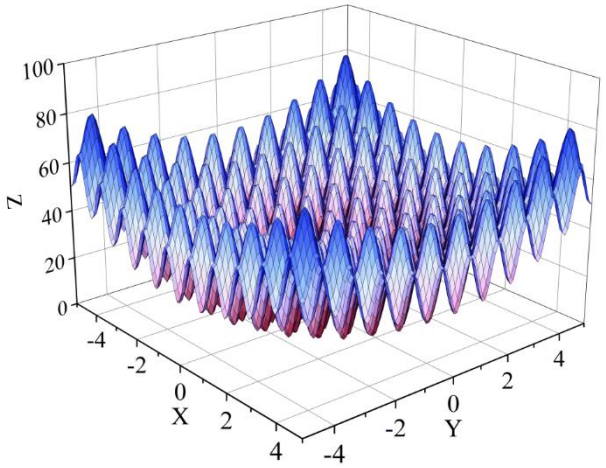

Figure 5: Rastrigin function

The formula which belongs to the Ackley function is just like what follows:

$$f(x)=-a\exp\left(-b\sqrt{\frac{1}{d}\sum_{i=1}^{d}x_i^2}\right)-\exp\left(\frac{1}{d}\sum_{i=1}^{d}\cos\left(cx_i\right)\right)+a+\exp(1) \tag{45}$$

The Ackley function is a multi-peak function, the function decreases rapidly near the origin, and the algorithm can easily fall into local optimality during the search. Its search space is $-30 \le x_i \le 30$, and the optimal solution of the function is: $\min\left(f\left(x_i \right) \right) = f(0) = 0$. Its MATLAB simulation image is shown in Figure 6.

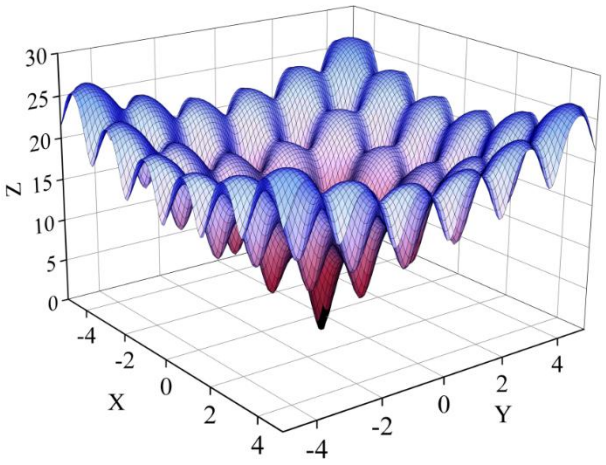

Figure 6: Ackley function

3.2 Feasibility analysis of hybrid algorithms

For verifying whether the IATAPSO algorithm which was put forward before has practicability, it is tested in this section using the Griewangk function.The expression of the Griewangk function is:

$$f(x) = \frac{1}{4000}\sum_{i=1}^{D} x_i^2 - \prod_{i=1}^{D} \cos\left(\frac{x_i}{\sqrt{i}} \right) + 1 \tag{46}$$

The Griewangk function is a representative multi-peak function which possesses a search domain of $-500 \le x_i \le 500$. The function has more local extreme points in this search space: $x_i \approx \pm k\pi\sqrt{i}, i = 1,2,3\cdots D$. The optimal solution of the function is $\min\left(f\left(x_i \right) \right) = f(0) = 0$. Its MATLAB simulation image is shown in Fig. 7.

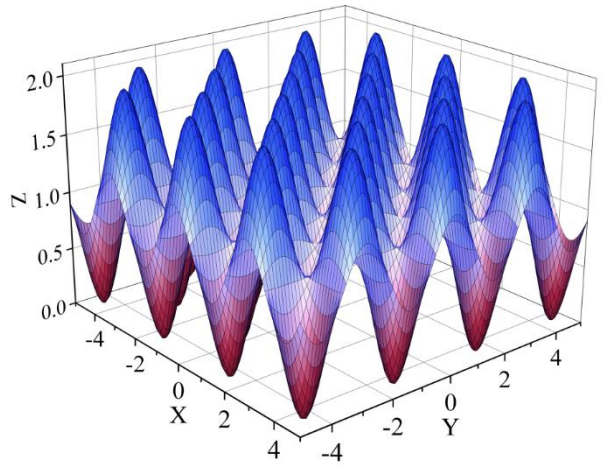

Figure 7: Griewangk function

Table 1 gives the arrangement of the parameters that the algorithm uses. In the process which enhances the algorithm, the adjustment that is made on parameter z can change the degree to which the taboo table participates in the procedure of algorithm optimization. This alteration brings influence to the population diversity of the algorithm, hence it also can affect both the probability that the algorithm achieves successful convergence and the efficiency of the convergence. In order to exclude errors due to chance factors in the iterative process, the function was tested for 30 times of optimization under different parameters, Furthermore, the average magnitude of the results connected to the quantity of repetition cases which the algorithm utilizes in the problem-solving process has been computed. Figure 8 has shown the relation diagram between iteration times and z-value when IATAPSO is used by us to optimize Griewangk function under different dimension conditions. At the same time, Figure 9 gives the drawing of the successful rate together with the z-value and the dimension D value for the optimization of the Griewangk function which is solved by IATAPSO.

Figure 8 shows us that when the dimension D of the query is not big, the chosen z-value brings an extremely tiny influence on the quantity of the algorithm iteration steps. This is because that the problem itself possesses a low degree of complexity.Along with the rising of problem dimensionality D, the complexity degree of the problem has an increase. Therefore, the quantity of repeated cycles which the algorithm requires to discover a solution goes up, and the impact of the selected z-value upon the iteration quantity of the algorithm also becomes more obvious. When the value of z is about 0.6, the algorithm that we use needs the smallest number of iteration steps. On the opposite side, if the z-value we set is too high, the multiplicity of the group is decreased to a certain extent. This decreasing of population diversity therefore causes a rising in the quantity of iteration times.

Figure 9 makes known that when the dimension D of the problem is comparatively small, the algorithm has a success rate that is close to 100% in the solving of the test function.When the problem dimension exceeds 40, the success rate of the algorithm's solution appears to decrease. The success rate which the algorithm obtains when it solves the function under the same problem dimension D has more obvious fluctuation along with the change of z value, and the algorithm has the highest success rate when $0.6<z<0.7$.

Table 1: Algorithm parameter setting

M	30
$gen_{\max}$	110
φ	0.5
u	0.5
α	0.5
μ	5
$j_{\max}$	5

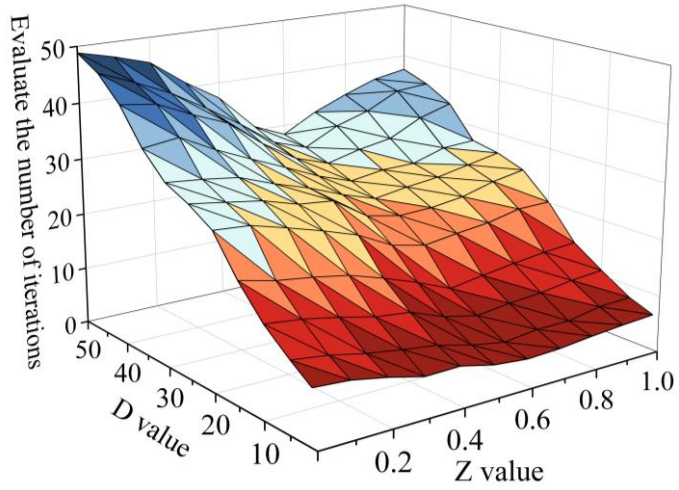

Figure 8: Iterations are changed with the Z and dimension D values

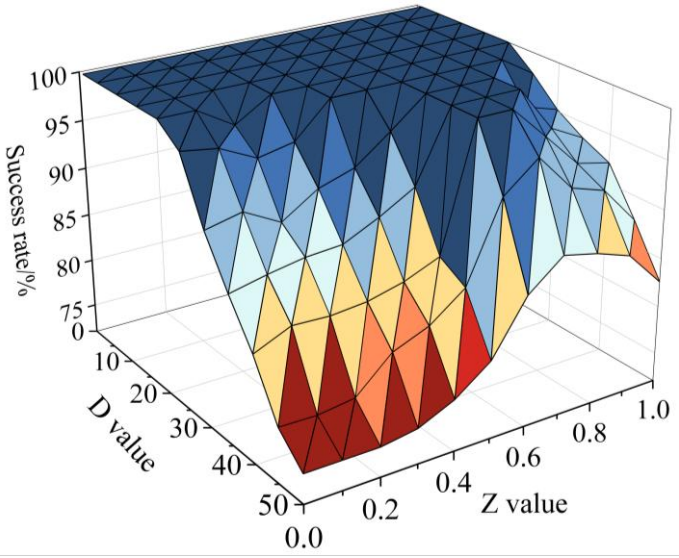

Figure 9: Success rate changes with the Z value and dimension D values

3.3 Hybrid Algorithm Performance Testing

Furthermore, the average size of the results connected with the count of repetition cases that the algorithm uses when the problem-solving process is going on has been computed. Figure 8 shows the relation drawing between the iteration count and the z-value when we use IATAPSO to carry out optimization for the Griewangk function under different dimension conditions. At the same time, Figure 9 gives the drawing of the successful rate together with the z numerical value and the dimension D numerical value for the optimization of the Griewangk function which is solved by IATAPSO.

Table 2 give the arrangement of parameters for the algorithm, hence Table 3 exhibit the parameter arrangements for every test function.

Table 2: Algorithm parameter setting

	PSO	IATAPSO
M	30	30
$gen_{\max}$	110	110
φ	0.5	0.5
u	0.5	0.5
α	0.5	0.5
μ	5	5
$j_{\max}$		5
z		0.5

Table 3: Test function parameter Settings

	Dimension/D	Search space	Minimum value	Target value
Sphere	20	[-80,80]	0	0.01
Rosenbrock	20	[-30,30]	0	0.01
Griewangk	20	[-500,500]	0	0.01
Rastrigin	20	[-5,5]	0	0.01
Ackley	20	[-30,30]	0	0.01

In order to exclude the error due to chance factors in the iterative process, the two algorithms are tested for 100 times of optimization search for different test functions, the main performance targets are recorded, and we carry out the computation of the average value of iteration counts. All the outcomes we have found are shown in Table 4. According to what we can discover clearly:

(1) In the $f\left(G_{best}\right)$ computation results of the test functions, IATAPSO's computation results for the first four test functions are all 0, while PSO falls into the local optimum in the computation of the last four test functions, and IATAPSO's ability of jumping out of the local optimum is significantly better than PSO.

(2) Because of the existence of the chaotic optimization step in IATAPSO, the particles are broken up when they are relatively concentrated, the $f\left(m_{best}\right)$ and standard deviation of IATAPSO are larger than that of PSO during the calculation of the test functions.

(3) When we carry out calculation for each test function, the iteration number and success proportion of the Improved Adaptive Time-varying Acceleration Particle Swarm Optimization (IATAPSO) are higher than those of the Particle Swarm Optimization (PSO). Furthermore, the search efficiency that the IATAPSO algorithm has is distinctly higher than what the PSO possesses.

Table 4: Compares performance indicators for standard test function tests

Test function	Algorithm	$f(G_{best})$	$f(m_{best})$	Standard deviation	Iteration number	Success rate
Sphere	PSO	0	4.537e -08	4.625e -09	29.49	1.00
	IATAPSO	0	0.0586	0.0175	7.80	1.00
Rosenbrock	PSO	5.334e -08	3.241e -06	9.418e -06	36.58	0.77
	IATAPSO	0	0.0088	8.910e -03	19.37	1.00
Griewangk	PSO	6.063e -06	1.419e -04	4.274e -05	27.34	0.54
	IATAPSO	0	1.093e -03	0.139	14.92	1.00
Rastrigin	PSO	8.166e -05	8.287e -06	6.201e -08	63.29	0.45
	IATAPSO	0	0.0361	1.811e -03	36.06	1.00
Ackley	PSO	0.045	0.545	6.288e -04	82.16	0.74
	IATAPSO	2.363e -04	0.6103	0.0771	41.23	0.87

4 Optimal capacity design and energy efficiency analysis

This research carries out the focusing on the X large-scale new-energy base, it conducts the deep delving and carries out the analyzing of the issue that belongs to energy-storage capacity configuration when the pre-planning phase is in process. Because the present research only discusses the capacity-configuration question of energy-storage equipment, the capacities of wind power stations, solar power plants, and the network framework are all predetermined values. First of all, we carry out an analysis upon the optimized operation of the energy-storage system, when the energy-storage capacity is set as 10MW/20MWh. According to the inner optimization outcomes, the service life of the energy-storage system is assessed through the use of the energy-storage system battery health-condition evaluation model. This procedure shows the changes which happen to the battery's health condition and the yearly net income of the energy-storage system in its whole life cycle. After that, the results of energy-storage capacity distribution are gotten modification. Production simulation works are then conducted through expanding the wind-power sampling data to confirm the optimal energy-storage distribution capability.

4.1 Basic data

We have carried out the selection of one sample which is for analysis. It is composed of the measured power values of wind and photovoltaic (PV) energy at the X energy base in the year 2024. The wind power station of this base holds a rated capacity of 250 megawatts (MW), hence the photovoltaic power station holds a rated capacity of 140 MW. The peak electric power of the local client load is 100 MW. For the convenience of carrying out the analysis of the results, the dispatch result of one single day is randomly selected to carry out the verification and assessment of the model that we put forward. Figure 10(a) and Figure 10(b) separately describe the output properties of wind and solar energy in the X energy base and the original load properties of this station. The time-of-use electricity price arrangement is placed in Table 5, and the parameter numerical values are displayed in Table 6. The normative on-grid electricity price for wind power is 0.37 yuan each kilowatt-hour, and the normative on-grid electricity price for centralized photovoltaic power is 0.38 yuan each kilowatt-hour.After we look at Figure 10, we can clearly see that the output of photovoltaic power generation changes along with the strength of sunlight, showing a rule of “high in the center and low at the two ends”. The peak strength of photovoltaic electricity generation is attained as 153.3 MW at the time of 14:00. In the time

period from 1 o'clock to 9 o'clock, and also from 20 o'clock to 24 o'clock, the production amount of solar electric power through photovoltaic technology reaches zero.The average every day electric quantity of photovoltaic electricity generation achieves 40.73 MW. On the opposite side, the power data that wind power generation produces has very obvious fluctuation phenomena. The minimum wind power output quantity is 11.96 MW which occurs at 18:00, while the maximum is 170.78 MW which occurs at 01:00. The average power output which wind power generation produces in the whole one day is equal to 62.26 megawatts.The random volatility of the power consumption of territorial loads, with the main loads concentrated in the period from 10:00 a.m. to 24:00 p.m., with the maximum power consumption of 96.39MW at 19:00, the minimum power consumption of 81.64MW at 04:00, and the average power of photovoltaic power generation for the whole day was 40.73MW. The maximum power consumption was 96.39MW at 19:00, the minimum power consumption was 81.64MW at 4:00, and the average power consumption for the whole day was 88.88MW.

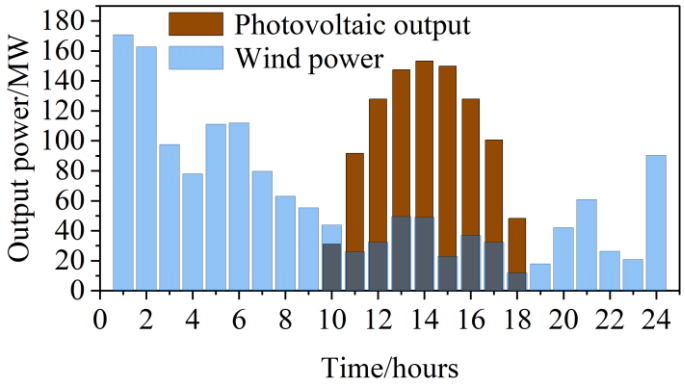

(a) Wind and solar power generation

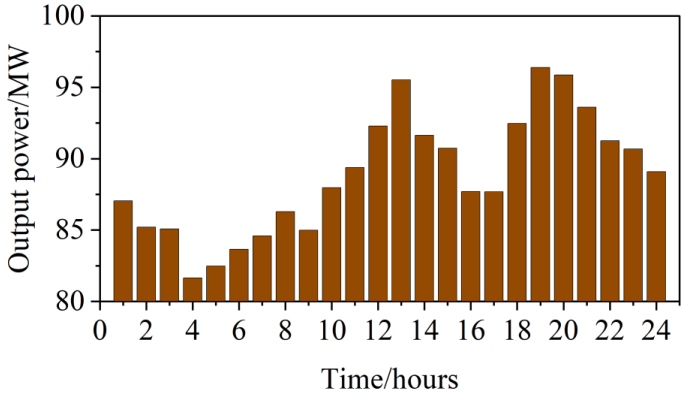

(b) Local load

Figure 10: Typical daily load curve and wind light

Table 5: Peak valley price

Hour	Hour	Electrovalence(Yuan/kWh)
Peak	7:00-9:00, 18:00-24:00	0.756
Flat	00:00-2:00, 4:00-7:00, 9:00-11:00, 17:00-18:00	0.507
Valley	2:00-4:00, 11:00-17:00	0.253

Table 6: Related parameters and control variable range

Parameter/Variable	Value/Range
Local coal plants are benchmarking for Internet prices (Yuan/kWh)	0.305
Wind power benchmarking (Yuan/kWh)	0.37
Photovoltaic benchmark Internet price (Yuan/kWh)	0.38
Energy storage unit capacity cost (Yuan/kWh)	630
Energy storage unit power cost (Yuan/kWh)	420
Energy storage unit transportation cost (Yuan/kWh)	0.06
$[SOC_{\min}, SOC_{\max}]$	[0.1,0.85]
Energy storage equipment initial SOC value	0.6
Carbon trading price (Yuan/kWh)	0.07
Contact line upgrade cost (Yuan/kWh)	8500
Battery replacement rate (%)	6
Expected yield (%)	9
Discount rate (%)	0.11
The value of the power volatility of the parallel network (%)	3.2

4.2 Analysis of optimized operation of energy storage systems

We may take the energy storage arrangement of 10 megawatts (MW) and 20 megawatt-hours (MWh) to be one example. After we carry out an analysis, therefore, we get the charge and discharge condition of the energy storage battery, which is shown in Figure 11. Our analysis makes clear that from 1:00 a.m. to 6:00 a.m., this is the time period in which the residential electricity use reaches its lowest level. At this time point, according to the time-divided electricity price, in the low-price period, the energy storage battery which is at the energy base obtains electric energy from the system to carry out charging. During 7 o'clock in the morning to 9 o'clock in the morning, this is the period that electricity price is peak. In this period, the energy-storing battery provides electric energy to the electric devices, and it is located in the discharging working stage. In the time period from 11:00 to 17:00, a process which is first charging and then discharging is undergone by the energy storage batteries. The principle which supports this is that the time interval from 11:00 to 17:00 is located inside the low electricity tariff period. In the time of 11 o'clock, the energy storage system cuts the capacity demand in order to obtain a bigger profit, reflected in the delay of the contact line expansion and reconstruction of the return at this time accounted for 66.2% of the total return of the year of commissioning,therefore, in order to reduce the demand for electric power of the contact line, the energy storage device at the present time is operated in the discharge mode, in 18:00-21:00 in the peak power consumption, energy storage battery discharge, but due to the latter two phases of the discharge power demand is larger, so the time period of energy storage discharge power is limited. The result gotten from the analysis shows that the mathematical model and algorithm which are put forward in this article have the ability to reach the optimal goal function.

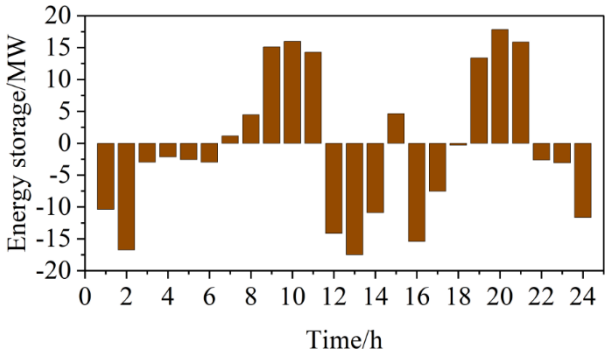

Figure 11: Storage system charge and discharge power

According to the charge and discharge performance characteristics of the energy-storage battery, the detailed state-of-charge (SOC) data of the energy-storage battery can be obtained, which is shown in Figure 12. In this situation, when the SOC presents a rising tendency, it thus shows that the battery is in the process of being charged. On the opposite side, a downward changing tendency of the SOC indicates that the battery is in the process of being discharged.

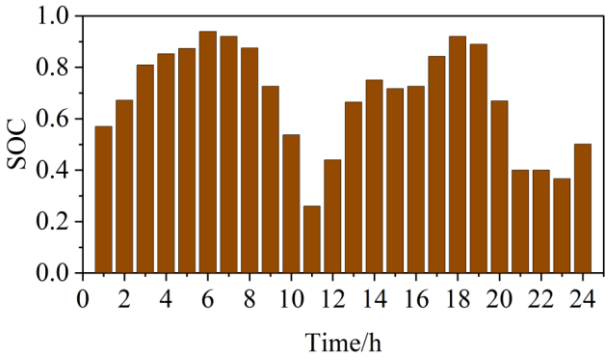

Figure 12: Energy storage for soc

According to the State-of-Charge (SOC) data of the energy storage device which begin from the year when it was put into operation, the residual capacity of the energy storage can be calculated. After this step, therefore, the storage capability can be updated to improve the SOC data of the energy storage devices for the next year. This process that data get updated is being conducted continuously. Therefore, the correlation between the operation years of energy storage equipment and its health state in the whole life cycle can be obtained, which is shown in Figure 13.

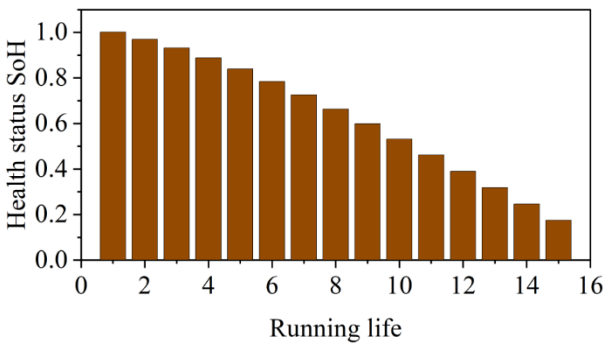

Figure 13: Storage battery health status change trend

From the battery's health situation, we can see that with the increment of working years, the battery's health condition has a gradual worsening trend. Till the 16th year, the healthy condition of the energy-storage battery has a fall below 20 percent. When the state of health (SoH) of battery drops lower than 20%, the battery just begins to be retired, this marks the finishing of its life cycle. Along with the increment of the number of working years, the service length of the accumulator cell decreases at an accelerating speed together with the passing of working years. Figure 14 shows the relation between the working life length of energy storage and the income in the entire life period.

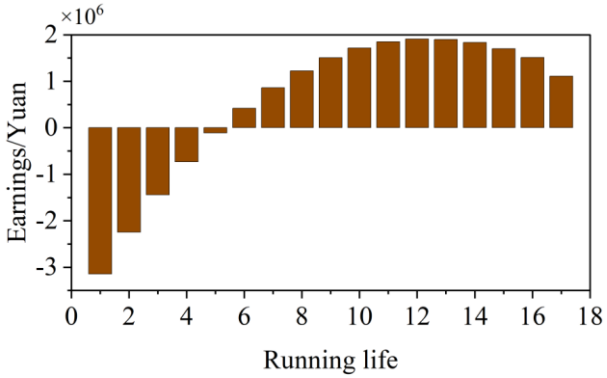

Figure 14: Trend of net income changes in storage cells

When the new energy base has gotten an energy storage capacity of 10MW/20MWh, the net profit only then starts to change from negative to positive in the sixth year of its operation. That is namely, the dynamic investment recycle time of the energy storage is about six years. The net profit achieves its peak in the twelfth year. After that, along with the increase of working years, the battery attenuation gradually becomes faster, hence it causes the profit to firstly go up and then go down. When the health state of battery falls below 20 percent, the net profit coming from energy storage investment therefore will decrease with a speed that becomes faster and faster. For the purpose of probing into the quantum of curtailed wind electric energy and solar electric energy in the electric power system both before and after the installment of energy storage equipment, we are capable of ascertaining the alteration of the wind and solar curtailment proportion before and after the arrangement deployment of energy storage. This thing is displayed in Figure 15. It is very obvious that after the constructing of energy storage is completed, there exists an obvious decrease in the quantity of curtailed wind and solar electric energy, with an average decreasing value of 66.84%.

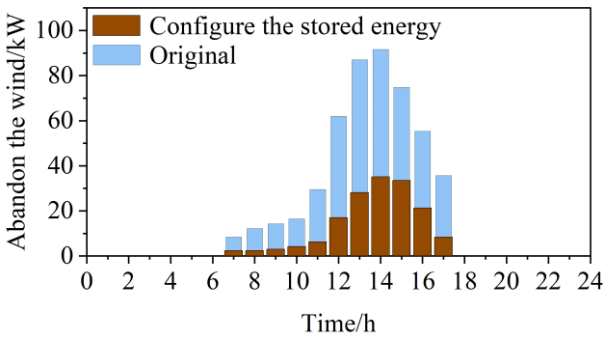

Figure 15: Abandon wind abandon light change

4.3 Analysis of results of capacity optimization allocation

Figure 16 shows the net benefit of a new energy field workstation when the capacity of the storage battery makes changes. At this place, the advantage stands for the accumulated profit through the whole life-cycle, 15MW can only run for 8 years, the benefit is the benefit of 8 years. 15-50MW can run for 9 years, the benefit is the benefit of 9 years, and so on.It is very clear that when the energy storage capability of the new-energy power plant increases, the net income at first has a going-up tendency and afterward begins to go down, this indicates therefore that the energy storage capacity is not necessarily more excellent when it has bigger size. Along with the promotion of storage capacity, it not only can increase the construction expense of the battery storage system but also can bring about the descent of operation efficiency.At present, the policy which is put forward about the proportion of energy storage in the construction of new-energy bases is situated in the scope of about 10% to 15%.Take as an example, in the situation of a new-energy base which has an optimal collocated capacity of 50MWh, the percentage of energy-storage disposition that relates to the new-energy installed capacity at this moment is 11.47%, at this time, the wind and light energy base of the power demand and the whole life cycle to achieve the maximum benefit.

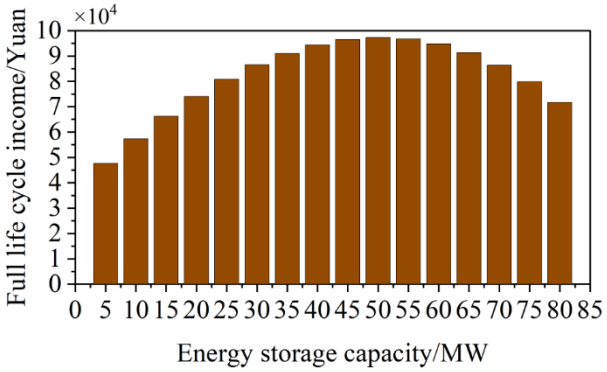

Figure 16: Changes in the capacity of the battery with the capacity of the battery

5 Conclusion

In this research, we have brought forward a two-phase optimization model which is prepared for the distribution of energy storage and the economic running of the system.In addition, a strengthened adaptive tabu-annealing particle swarm algorithm is designed by us for solving this model. When we carry out calculation on every test function, the iteration quantity and the success rate of the improved adaptive tabu-annealing particle swarm algorithm (IATAPSO) are all better than those which belong to the particle swarm optimization (PSO) algorithm.It is worth noting that the efficiency of the searching process of this algorithm is obviously higher than the efficiency which the PSO has.The computation results of IATAPSO for the Sphere, Rosenbrock, Griewangk, and Rastrigin test functions are all 0, while PSO in Rosenbrock, Griewangk, Rastrigin, and Ackley test functions all fall into local optimization, and IATAPSO's ability to jump out of local optimization is obviously better than PSO.

The present research has chosen the large-scale new-energy base X to be the object which is studied by this work. This paper carries out computation by utilizing the distribution method which optimizes capacity, for the wind-photovoltaic-energy-storage complementary system which this paper puts forward. When we set energy storage capacity to 10MW/20MWh, compared with the old energy-storage arrangement, the system’s wind and solar energy curtailment has a very obvious reduction. By average calculation, the curtailment degree has

been reduced by 66.84%. Under the background of the electric power requirement and the entire life cycle of the wind and solar energy base, for obtaining the biggest profit, the optimal configuration capacity of the new energy base is equal to 50 megawatt-hours.Furthermore, the proportion of energy-storage arrangement occupies 11.47 percent of the installed new-energy capacity.

About the Author

Chenguang Zhu was born in 1984 in Pingdingshan, Henan, China.He has already gotten the master diploma in the electric engineering domain. In the current time, he holds the post of the head of the Pinggao Comprehensive Energy Research Institute, is responsible for the research and development of the overall scheme design.

Min Gao was born in Pingdingshan, Henan, P.R. China, in 1992. She graduated from North China University of Water Resources and Electric Power in 2015 with a bachelor's degree. Now, she works in Pinggao Group Co., Ltd. Her research interests include energy management and new energy planning and design.

Xiaojun Si was born in February 1984. He holds a bachelor's degree in Computer Science and Technology. Currently, he works in Pinggao Group Co., Ltd., where he is responsible for market research and promotion.

Qunwei Gao, born in 1983, Pingdingshan, Henan, P.R. China, he graduated from Electrical engineering and holds the title of senior engineer. His current work is mainly responsible for edge computing technology research and development and practice.

Weizhe Sun, who was given birth in 1995 at Pingdingshan City, Henan Province, finished his learning at Zhengzhou University of Light Industry. In current time, he holds a work position in the comprehensive energy branch of Pinggao Group. His main research directions include computer software, computer application, comprehensive energy, and electric power industry.

References

[1] Zissler, R. (2022). During the energy crisis renewable energy grows, fossils and nuclear energy decrease. Renewable Energy Law and Policy Review, 11(1), 28-31.

[2] Bilgili, M., Tumse, S., & Nar, S. (2024). Comprehensive overview on the present state and evolution of global warming, climate change, greenhouse gasses and renewable energy. Arabian Journal for Science and Engineering, 49(11), 14503-14531.

[3] Zile, M. (2018). Implementation of solar and wind energy by renewable energy resources with fuzzy logic. International Journal on Technical and Physical Problems of Engineering (IJTPE), (34), 46-51.

[4] Li, Y., Huang, X., Tee, K. F., Li, Q., & Wu, X. P. (2020). Comparative study of onshore and offshore wind characteristics and wind energy potentials: A case study for southeast coastal region of China. Sustainable Energy Technologies and Assessments, 39, 100711.

[5] Qiu, T., Wang, L., Lu, Y., Zhang, M., Qin, W., Wang, S., & Wang, L. (2022). Potential assessment of photovoltaic power generation in China. Renewable and Sustainable Energy Reviews, 154, 111900.

[6] Weschenfelder, F., Leite, G. D. N. P., da Costa, A. C. A., de Castro Vilela, O., Ribeiro, C.

M., Ochoa, A. A. V., & Araújo, A. M. (2020). A review on the complementarity between grid-connected solar and wind power systems. Journal of Cleaner Production, 257, 120617.

[7] Ding, Z., Hou, H., Yu, G., Hu, E., Duan, L., & Zhao, J. (2019). Performance analysis of a wind-solar hybrid power generation system. Energy Conversion and Management, 181, 223-234.

[8] Couto, A., & Estanqueiro, A. (2021). Assessment of wind and solar PV local complementarity for the hybridization of the wind power plants installed in Portugal. Journal of Cleaner Production, 319, 128728.

[9] Devrim, Y., & Eryilmaz, S. (2021). Reliability-based evaluation of hybrid wind–solar energy system. Proceedings of the Institution of Mechanical Engineers, Part O: Journal of Risk and Reliability, 235(1), 136-143.

[10] Roy, P., He, J., Zhao, T., & Singh, Y. V. (2022). Recent advances of wind-solar hybrid renewable energy systems for power generation: A review. IEEE Open Journal of the Industrial Electronics Society, 3, 81-104.

[11] Babaremu, K., Olumba, N., Chris-Okoro, I., Chuckwuma, K., Jen, T. C., Oladijo, O., & Akinlabi, E. (2022). Overview of solar–wind hybrid products: Prominent challenges and possible solutions. Energies, 15(16), 6014.

[12] Abdelghany, M. B., Al-Durra, A., & Gao, F. (2023). A coordinated optimal operation of a grid-connected wind-solar microgrid incorporating hybrid energy storage management systems. IEEE Transactions on Sustainable Energy, 15(1), 39-51.

[13] de Doile, G. N. D., Rotella Junior, P., Rocha, L. C. S., Bolis, I., Janda, K., & Coelho Junior, L. M. (2021). Hybrid wind and solar photovoltaic generation with energy storage systems: A systematic literature review and contributions to technical and economic regulations. Energies, 14(20), 6521.

[14] Xiao, B., Gao, Z., Peng, H., Chen, K., Li, Y., & Liu, K. (2023). Robust optimization of large-scale wind–solar storage renewable energy systems considering hybrid storage multi-energy synergy. Sustainability, 16(1), 243.

[15] Suo, X., Zhao, S., Ma, Y., & Dong, L. (2021). New energy wide area complementary planning method for multi-energy power system. IEEE Access, 9, 157295-157305.

[16] Zhu, Y., He, Y., & Zhou, Q. (2025). Impact of multi-energy complementary system on carbon emissions: Insights from a rural building in Shangluo City, China. Energy Conversion and Management, 327, 119595.

[17] Zhu, R., Zhao, A. L., Wang, G. C., Xia, X., & Yang, Y. (2020). An Energy Storage Performance Improvement Model for Grid-Connected Wind-Solar Hybrid Energy Storage System. Computational Intelligence and Neuroscience, 2020(1), 8887227.

[18] Hou, H., Xu, T., Wu, X., Wang, H., Tang, A., & Chen, Y. (2020). Optimal capacity configuration of the wind-photovoltaic-storage hybrid power system based on gravity energy storage system. Applied energy, 271, 115052.

[19] Ma, X., Deveci, M., Yan, J., & Liu, Y. (2024). Optimal capacity configuration of wind-photovoltaic-storage hybrid system: A study based on multi-objective optimization and sparrow search algorithm. Journal of Energy Storage, 85, 110983.

[20] Liu, M., Shen, S., & Wang, W. (2025). Capacity configuration optimization of wind-solar-storage systems in park microgrids considering lifecycle carbon emission. Journal of Renewable and Sustainable Energy, 17(5).

[21] Zheng, Y., Wang, S., Liu, C., Shen, C., & Liu, J. (2025). Capacity optimization of wind-solar complementary hybrid energy storage system combining GWO and PIO. Engineering Research Express, 7(4), 045359.

[22] Wang, Y., Ji, H., Luo, R., Liu, B., & Wu, Y. (2025). Energy Optimization Strategy for Wind–Solar–Storage Systems with a Storage Battery Configuration. Mathematics, 13(11), 1755.

[23] Wu, X., Xu, K., Wang, Z., & Gong, Y. (2017, November). Optimized capacity configuration of an integrated power system of wind, photovoltaic and energy storage device based on improved particle swarm optimizer. In 2017 IEEE Conference on Energy Internet and Energy System Integration (EI2) (pp. 1-6). IEEE.

[24] Qian, S. U. N., Jianwei, M. A., Yanjie, S. H. E., Jingchao, Z. H. A. N. G., Bo, G. U., & Zichao, Z. H. A. N. G. (2019). Optimal Configuration of Standalone Wind-Solar-Storage Complementary Generation System Based on the GA-PSO Algorithm. Journal of Power Technologies, 99(4).

[25] Lv, M., Gou, K., Chen, H., Lei, J., Zhang, G., & Liu, T. (2024). Optimal Design of Wind-Solar complementary power generation systems considering the maximum capacity of renewable energy. Energy, 312, 133650.

[26] Wang, B., Wu, L., Zhang, P., Gu, Y., Zhang, F., & Guo, J. (2025). Capacity Configuration Optimization of Wind–Light–Load Storage Based on Improved PSO. Energies, 18(19), 5212.

[27] Jiang, Z., Gao, J., Zhu, Y., Cao, Y., Wang, X., & Zhong, F. (2025, July). Research on Capacity Allocation of Wind-Solar Hybrid Energy Storage Microgrid Based on Improved Particle Swarm Optimization. In 2025 International Conference of Clean Energy and Electrical Engineering (ICCEEE) (pp. 1-6). IEEE.